

Ultrafast Photoinduced Electron Transfer in Green Fluorescent Protein Bearing a Genetically Encoded Electron Acceptor

Xiaoxuan Lv,^{†,||} Yang Yu,^{§,||} Meng Zhou,[‡] Cheng Hu,[†] Feng Gao,[†] Jiasong Li,[†] Xiaohong Liu,[†] Kai Deng,[†] Peng Zheng,[†] Weimin Gong,[†] Andong Xia,^{*,‡} and Jiangyun Wang^{*,†}

[†]Laboratory of RNA Biology and Laboratory of Quantum Biophysics, Institute of Biophysics, Chinese Academy of Sciences, 15 Datun Road, Chaoyang District, Beijing 100101, China

[‡]Institute of Chemistry, Chinese Academy of Sciences, Beijing 100190, China

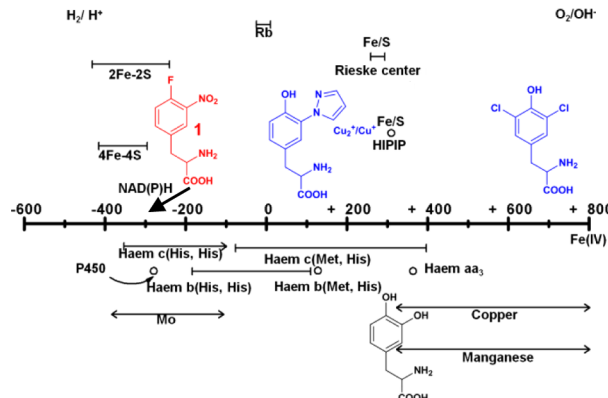
[§]Department of Chemistry, University of Illinois at Urbana–Champaign, Urbana, Illinois 61801, United States

 Supporting Information

ABSTRACT: Electron transfer (ET) is widely used for driving the processes that underlie the chemistry of life. However, our abilities to probe electron transfer mechanisms in proteins and design redox enzymes are limited, due to the lack of methods to site-specifically insert electron acceptors into proteins *in vivo*. Here we describe the synthesis and genetic incorporation of 4-fluoro-3-nitrophenylalanine (FNO_2Phe), which has similar reduction potentials to NAD(P)H and ferredoxin, the most important biological reductants. Through the genetic incorporation of FNO_2Phe into green fluorescent protein (GFP) and femtosecond transient absorption measurement, we show that photoinduced electron transfer (PET) from the GFP chromophore to FNO_2Phe occurs very fast (within 11 ps), which is comparable to that of the first electron transfer step in photosystem I, from P700* to A_0 . This genetically encoded, low-reduction potential unnatural amino acid (UAA) can significantly improve our ability to investigate electron transfer mechanisms in complex reductases and facilitate the design of miniature proteins that mimic their functions.

The chemistry of life processes, most notably photosynthesis, are driven largely through the directional movement of electrons in proteins.^{1–18} While natural amino acids (such as cysteine, tyrosine, and tryptophan) can serve as electron donors, they are not known to be used as electron acceptors.^{19–24} To facilitate efficient electron transfer in living systems, nature has employed numerous metal-containing electron-accepting cofactors such as iron–sulfur clusters, copper, and haem, which have broadly tunable redox potentials (Scheme 1 and Figure S1).^{1,25–33} For example, three iron–sulfur clusters are present in photosystem I (PI), which together form a facile electron accepting route to the photochemical reduction of $\text{NAD}(\text{P})^+$ to produce $\text{NAD}(\text{P})\text{H}$.²⁵ However, the factors controlling the redox potentials of metal cofactors are still poorly understood, and it is difficult to introduce metal binding sites with desirable redox potentials into proteins.^{34–36} Furthermore, the mechanism of metal-cofactor insertion into proteins *in vivo* is extremely complicated and remains an important frontier of bioinorganic chemistry.³⁷

Scheme 1. Redox Potential Range of Various Metal Cofactors (in Millivolts, versus the Standard Hydrogen Electrode) in Proteins and Genetically Encoded Unnatural Amino Acids^a



^aThe structure of 4-fluoro-3-nitrophenylalanine, which is reported in this work, is highlighted in red.

New methods for the genetic incorporation of metal-independent redox probes with various reduction potentials greatly expand our ability to investigate electron transfer mechanism in proteins,³⁸ design oxidases and reductases,³⁹ and construct photoinduced electron transfer (PET) fluorescent sensors,⁴⁰ *in vivo* and *in vitro*. In previous works, we and others have reported the genetic incorporation of the unnatural amino acids (UAA) 3,5-dichlorotyrosine (Cl_2Y), 3,5-difluorotyrosine- (F_2Y),^{38,40} and Dopa,³⁹ which have redox potentials spanning from 400 to 800 mV. While we have demonstrated that upon Cu(II) binding the genetically encoded UAA 3-pyrazole-tyrosine(pyTyr)⁴¹ can be used as an efficient electron acceptor, the reduction potential of the pyTyr/Cu(II) complex (168 mV) is much higher than NAD(P)H and therefore precludes the design of reductases.⁴²

In this work, we describe the facile synthesis and genetic incorporation of 4-fluoro-3-nitrophenylalanine (FNO_2Phe , or FN) 1. The crystal structure of the *Aequorea victoria* green fluorescent protein (GFP) bearing FNO_2Phe at a specific site

Received: April 8, 2015

Published: May 28, 2015

(Figure 2) reveals that the small size of the FNO₂Phe does not cause significant structural changes to GFP.

Through femtosecond transient absorption measurement, we establish that electron transfer from the GFP chromophore to FNO₂Phe occurs very fast, within 11 ps, in a distance-dependent manner. This rate is comparable to that of the first electron transfer step in photosystem I, from P700* to A₀, which occurs within 10–30 ps after P700 photoexcitation⁴³ (Figure S2). The GFP mutants bearing FNO₂Phe reported in this work recapitulate two important properties of photosystem I: very fast forward electron transfer rate and photoinduced production of strongly reducing species. Further development along this route may result in miniature protein systems, which recapitulate the most important property of PS I, the photocatalytic production of NAD(P)H.

The UAAs FNO₂Phe and NO₂Phe (Scheme S1)^{45–47} have peak potentials comparable to that of the iron–sulfur clusters and NAD(P)H at −310 and −470 mV, respectively, as shown by cyclic voltammetry measurements (Figure S8).⁴⁴ FNO₂Phe was synthesized in two steps using a previously reported method with minor modifications (Scheme S1).⁴⁸ To selectively incorporate FNO₂Phe at specific sites in proteins produced in *E. coli*, a mutant *Methanocaldococcus jannaschii* tyrosyl amber suppressor tRNA (*MjtRNA*^{Tyr}_{CUA})/tyrosyl-tRNA synthetase (*MjTyrRS*) pair was evolved to incorporate FNO₂Phe in response to the TAG codon, as previously reported.⁴⁹ One *MjTyrRS* clone emerged after three rounds of positive selection and two rounds of negative selection. This clone was named FNO₂PheRS (Table S1).

To determine whether FNO₂PheRS can facilitate the incorporation of FNO₂Phe into proteins with high efficiency and fidelity, an amber stop codon was substituted for residue Ser4 in sperm whale myoglobin or Tyr151 in GFP. Protein synthesis was carried out in *E. coli* in the presence of UAA specific TyrRS mutants, *MjtRNA*^{Tyr}_{CUA} and 1 mM UAA, or in the absence of UAA as a negative control. Analysis of the purified protein by SDS-PAGE showed that full-length myoglobin and GFP expressed only in the presence of FNO₂Phe (Figure 1), indicating that FNO₂PheRS was specifically active for FNO₂Phe but inactive for any natural amino acids. The yields of mutant myoglobin and GFP were 10 and 20 mg/L, respectively. For

comparison, the yields of wild-type sperm whale myoglobin (wtMb) and GFP were 50 and 100 mg/L, respectively. ESI-MS analysis of FNO₂Phe encoded mutant GFP (GFP151FNO₂Phe) gave average masses of 27 756 Da, in agreement with the calculated mass (Figure 1C). The N-terminus methionine is cleaved, one water molecule and two hydrogen atoms are lost during chromophore maturation. Subsequent tryptic digestion and tandem mass spectrometric analysis confirmed the presence of FNO₂Phe at position 151 of the GFP (Figure S4). The high-resolution crystal structure of GFP151FNO₂Phe shows that the replacement of Tyr151 by FNO₂Phe causes little perturbation to the overall structure of GFP (Figure 2). The fluorine atom and

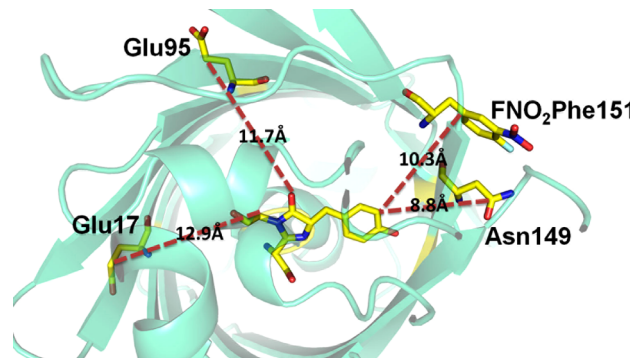


Figure 2. Crystal structure of the GFP151FNO₂Phe complex (PDB code: 4ON8). The GFP chromophore and residues 151, 149, 95, and 17 are shown as sticks.

nitro group are coplanar with the benzene ring. The planar structure of FNO₂Phe should be favorable for minimizing reorganization energy upon 1 electron reduction since the nitrobenzene anion radical also has a planar structure.⁴⁶

We then measured the relative fluorescence intensity of 5 μM wild-type GFP, GFP151FNO₂Phe, and GFP151NO₂Phe. As shown in Figure S6, GFP151FNO₂Phe exhibited 66% quenching compared to wild-type GFP. By contrast, GFP151NO₂Phe showed less than 5% quenching (see Figure S6). Since the absorption spectrum of FNO₂Phe does not overlap with the emission spectrum of GFP (see Figure S7), the fluorescence quenching is not caused by fluorescence resonance energy transfer (FRET). The difference in quenching can be explained by the difference in reduction potentials between FNO₂Phe and NO₂Phe. The reduction potential of FNO₂Phe is 160 mV lower than that of NO₂Phe, so there is a stronger driving force for PET from the GFP chromophore to FNO₂Phe, resulting in stronger quenching than is observed for NO₂Phe. We therefore chose FNO₂Phe for all our subsequent investigations.

To analyze the rate and distance-dependence of PET between the GFP chromophore and the electron accepting FNO₂Phe, femtosecond transient absorption measurements of wtGFP and GFP mutants were performed using a 400 nm pump laser. FNO₂Phe alone has no absorption at 400 nm (Figure S7). The transient absorption spectrum of wtGFP fits well to a sequential model (Scheme S2), with two components having decay times of ~1.3 ps and ~3.0 ns (Figure 3A and Table S2), consistent with previous investigations.^{50–53} These results indicate that after photoexcitation of the protonated neutral GFP chromophore deprotonation occurs within 1.3 ps, resulting in the formation of anionic I* with an excited-state absorption (ESA) around 440 nm and a stimulated emission (SE) around 509 nm.

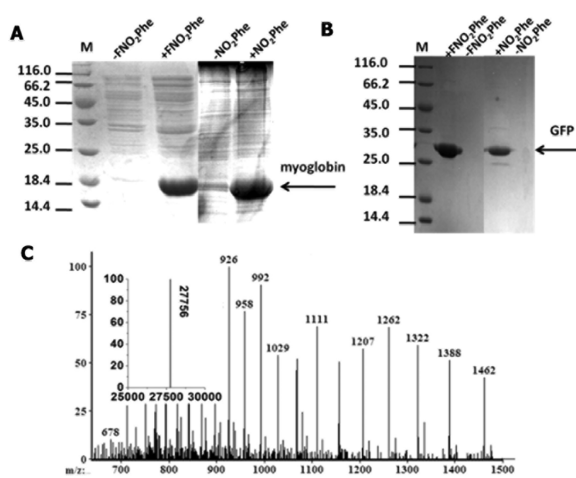


Figure 1. Coomassie-stained SDS-PAGE of TAG4 mutants myoglobin (A) or TAG151 mutants GFP (B) expressed in the presence or absence of 1 mM UAA. (C) ESI-MS spectra of the GFP151FNO₂Phe mutant. The inset shows the deconvoluted spectrum. Expected mass, 27 756 Da; observed mass, 27 756 Da.

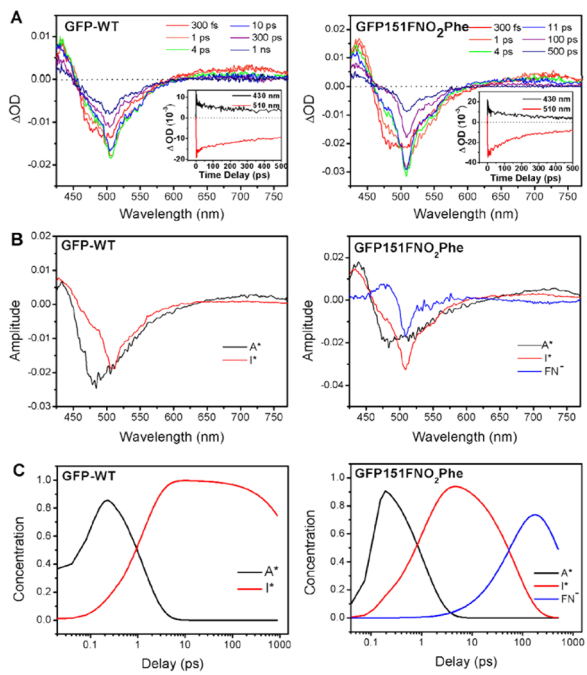


Figure 3. (A) Evolution of the transient absorption spectra of wtGFP and GFP151FNO₂Phe. The spectra are obtained at different delay times (pump at 400 nm). The inset shows the kinetic traces at specific wavelengths. (B) Species associated difference spectra (SADS) and (C) time-dependent concentrations of transient species obtained from target global fitting combined with singular value decomposition (SVD).

The ESA and SE of GFP151FNO₂Phe show a fast decay compared to the wtGFP (Figure 3), indicating efficient electron transfer from the GFP chromophore to FNO₂Phe. To extract the electron transfer rate, a kinetic scheme shown in Scheme S2 is proposed, which indicates electron transfer from I* to FNO₂Phe to yield the FNO₂Phe anion radical (FN⁻).

A target global fitting procedure based on the proposed kinetic model combined with singular value decomposition (SVD)^{50–54} was then employed to extract the time-dependent concentrations of transient species and species associated difference spectra (SADS)^{50–54} from the transient data as shown in Figure 3. The fitted time constants of wtGFP and GFP mutants are listed in Table S2. Besides the 1.8 ps excited state deprotonation reaction from A* to I* and a 3.2 ns decay from I* to ground state, a new decay process with a time-constant of 73 ps was obtained, resulting from the electron transfer from the GFP chromophore to FNO₂Phe. Our SADS data (Figure 3B) suggests the formation of the FNO₂Phe anion radical since a new peak around 470 nm appeared in GFP151FNO₂Phe, but not in wtGFP. This is consistent with previous electrochemical studies, which have reported that the nitrobenzene anion radical has absorbance maxima around 470 nm.⁵⁵ Furthermore, the similar transient absorption spectra of GFP149FNO₂Phe, GFP95FNO₂Phe, and GFP17FNO₂Phe are given in Figure S9, and the time-dependent concentrations of transient species and species associated difference spectra (SADS) are also extracted based on the same kinetic model as shown in Scheme S2. The fitted time constants of these GFP mutants are also listed in Table S2. In order to show the quality of fitting, kinetics at several selected wavelengths are plotted together with a global fit of all the collected time traces (Figure S10).

Based on the electron transfer time constants (τ_{ET}) of GFP-FNO₂Phe mutants obtained from the fitting procedure (see

Figure S10 and Table 1), we are able to calculate the electron transfer rate from the GFP chromophore to FNO₂Phe ($k_{ET} = 1/\tau_{ET}$).

Table 1. Distance-Dependent Electron Transfer Rate of wtGFP and Mutants

mutant	τ_{ET} (ps)	distance (Å)	k_{ET} (s ⁻¹)
GFP149FNO ₂ Phe	11 ± 0.55	8.8	(9.09 ± 0.45) × 10 ¹⁰
GFP151FNO ₂ Phe	73 ± 3.5	10.3	(1.37 ± 0.07) × 10 ¹⁰
GFP95FNO ₂ Phe	183 ± 11	11.7	(5.46 ± 0.33) × 10 ⁹
GFP17FNO ₂ Phe	253 ± 13	12.9	(3.95 ± 0.20) × 10 ⁹

τ_{ET}).⁵⁶ GFP149FNO₂Phe gives the shortest electron transfer time constant of 11 ps, which corresponds to an electron transfer rate constant of 9.09×10^{10} s⁻¹. The ET rate constants of GFP151FNO₂Phe, GFP17FNO₂Phe, and GFP95FNO₂Phe were slower, at 1.37×10^{10} , 5.46×10^9 , and 3.95×10^9 s⁻¹, respectively. The edge-to-edge distance from the GFP chromophore to residue FNO₂Phe 151 was 10.3 Å, according to the GFP151FNO₂Phe structure (Figure 2). Edge-to-edge distances from the GFP chromophore to residues FNO₂Phe149, FNO₂Phe17, and FNO₂Phe95 were estimated by measuring the shortest distance between the GFP chromophore and the β -carbons of residues Asn149, Glu17, and Glu95, respectively (Figure 2).^{57–60} Taken together these results demonstrate that PET from the GFP chromophore to FNO₂Phe can occur and that the rate of PET decreases exponentially as distance increases (Table 1).⁵⁷ The distance decay factor ($\beta = 0.9$ Å⁻¹) is close to that of a single-step tunneling reaction (Figure S11).^{58,59}

In conclusion, we have demonstrated the genetic incorporation of FNO₂Phe as an efficient electron accepting probe, which has reduction potential similar to that of iron–sulfur clusters and NAD(P)H. This new probe is well-suited for investigating electron transfer mechanism for reductases, such as photosystem I, hydrogenase, sulfite (nitrite) reductase, and nitrogenase, thus facilitating the design of miniature proteins mimicking their functions. In these complex enzymes, multistep electron hopping through iron–sulfur clusters is employed to optimize electron transfer rates. Since it is difficult to incorporate iron–sulfur cluster in designed metalloenzymes,⁶¹ the genetically coded FNO₂Phe may provide a suitable alternative for designing complex metalloenzymes. The fluorine atom on FNO₂Phe should also be helpful for EPR and NMR assignments for electron transfer studies.

Using this new method and femtosecond transient absorption measurement, we demonstrated that photoinduced electron transfer (PET) between green fluorescent protein (GFP) chromophore and protein-bound electron acceptor can occur rapidly, within 11 ps, suggesting that GFP may be optimized for PET reaction.

ASSOCIATED CONTENT

S Supporting Information

Methods. This material is available free of charge via the The Supporting Information is available free of charge on the ACS Publications website at DOI: 10.1021/jacs.Sb03652.

AUTHOR INFORMATION

Corresponding Authors

*andong@iccas.ac.cn

*jwang@ibp.ac.cn

Author Contributions

†These authors contributed equally to this work.

Notes

The authors declare no competing financial interest.

ACKNOWLEDGMENTS

We gratefully acknowledge the Major State Basic Research Program of China (2015CB856203), the National Science Foundation of China (21325211, 91313301, 21333012), CAS grant (KJZD-EW-L01), Innovation Fund For Technology Based Firms (14C26211100178) and Tianjin Municipal Grant (Y1M6101241). We thank Xiang Ding at the Core Facility for Protein Research, CAS for MS spectrum.

REFERENCES

- (1) Wasielewski, M. R. *Chem. Rev.* **1992**, *92*, 435.
- (2) Moser, C. C.; Keske, J. M.; Warncke, K.; Farid, R. S.; Dutton, P. L. *Nature* **1992**, *355*, 796.
- (3) Migliore, A.; Polizzi, N. F.; Therien, M. J.; Beratan, D. N. *Chem. Rev.* **2014**, *114*, 3381.
- (4) Cordes, M.; Giese, B. *Chem. Soc. Rev.* **2009**, *38*, 892.
- (5) Winkler, J. R.; Gray, H. B. *Chem. Rev.* **2014**, *114*, 3369.
- (6) Barber, J.; Andersson, B. *Nature* **1994**, *370*, 31.
- (7) Schultz, D. M.; Yoon, T. P. *Science* **2014**, *343*, 985.
- (8) Skourtis, S. S.; Beratan, D. N. *Science* **2007**, *316*, 703.
- (9) Wang, H. Y.; Lin, S.; Allen, J. P.; Williams, J. C.; Blankert, S.; Laser, C.; Woodbury, N. W. *Science* **2007**, *316*, 747.
- (10) Genereux, J. C.; Barton, J. K. *Chem. Rev.* **2010**, *110*, 1642.
- (11) Hammes-Schiffer, S.; Stuchebrukhov, A. A. *Chem. Rev.* **2010**, *110*, 6939.
- (12) Giese, B.; Gruber, M.; Cordes, M. *Curr. Opin. Chem. Biol.* **2008**, *12*, 755.
- (13) Merino, E. J.; Boal, A. K.; Barton, J. K. *Curr. Opin. Chem. Biol.* **2008**, *12*, 229.
- (14) Seefeldt, L. C.; Hoffman, B. M.; Dean, D. R. *Curr. Opin. Chem. Biol.* **2012**, *16*, 19.
- (15) Balzani, V.; Credi, A.; Venturi, M. *Curr. Opin. Chem. Biol.* **1997**, *1*, 506.
- (16) Boekema, E. J.; van Breemen, J. F.; van Roon, H.; Dekker, J. P. *Biochemistry* **2000**, *39*, 12907.
- (17) Stewart, D. H.; Nixon, P. J.; Diner, B. A.; Brudvig, G. W. *Biochemistry* **2000**, *39*, 14583.
- (18) Vasil'ev, S.; Bruce, D. *Biochemistry* **2000**, *39*, 14211.
- (19) Liu, Z.; Tan, C.; Guo, X.; Li, J.; Wang, L.; Sancar, A.; Zhong, D. *Proc. Natl. Acad. Sci. U.S.A.* **2013**, *110*, 12966.
- (20) Liu, Z.; Zhang, M.; Guo, X.; Tan, C.; Li, J.; Wang, L.; Sancar, A.; Zhong, D. *Proc. Natl. Acad. Sci. U.S.A.* **2013**, *110*, 12972.
- (21) Shih, C.; Museth, A. K.; Abrahamsson, M.; Blanco-Rodriguez, A. M.; Di Bilio, A. J.; Sudhamsu, J.; Crane, B. R.; Ronayne, K. L.; Towne, M.; Vlcek, A.; Richards, J. H.; Winkler, J. R.; Gray, H. B. *Science* **2008**, *320*, 1760.
- (22) Doose, S.; Neuweiler, H.; Sauer, M. *ChemPhysChem* **2009**, *10*, 1389.
- (23) Dutta, P. K.; Lin, S.; Loskutov, A.; Levenberg, S.; Jun, D.; Saer, R.; Beatty, J. T.; Liu, Y.; Yan, H.; Woodbury, N. W. *J. Am. Chem. Soc.* **2014**, *136*, 4599.
- (24) Gritsch, P. J.; Leitner, C.; Pfaffenbach, M.; Gaich, T. *Angew. Chem., Int. Ed.* **2014**, *53*, 1208.
- (25) Osyczka, A.; Moser, C. C.; Daldal, F.; Dutton, P. L. *Nature* **2004**, *427*, 607.
- (26) Mayo, S. L.; Ellis, W. R.; Crutchley, R. J.; Gray, H. B. *Science* **1986**, *233*, 948.
- (27) Park, J. S.; Karnas, E.; Ohkubo, K.; Chen, P.; Kadish, K. M.; Fukuzumi, S.; Bielawski, C. W.; Hudnall, T. W.; Lynch, V. M.; Sessler, J. L. *Science* **2010**, *329*, 1324.
- (28) Beinert, H.; Holm, R. H.; Munck, E. *Science* **1997**, *277*, 653.
- (29) Liu, J.; Chakraborty, S.; Hosseinzadeh, P.; Yu, Y.; Tian, S. L.; Petrik, I.; Bhagi, A.; Lu, Y. *Chem. Rev.* **2014**, *114*, 4366.
- (30) Rivalta, I.; Brudvig, G. W.; Batista, V. S. *Curr. Opin. Chem. Biol.* **2012**, *16*, 11.
- (31) Tobin, P. H.; Wilson, C. J. *J. Am. Chem. Soc.* **2014**, *136*, 1793.
- (32) Yu, F. T.; Penner-Hahn, J. E.; Pecoraro, V. L. *J. Am. Chem. Soc.* **2013**, *135*, 18096.
- (33) J. J. Fraustó da Silva, Williams, R. J. P. *The Biological Chemistry of the Elements*; Oxford University Press: Oxford, U.K., 2001.
- (34) Liu, J.; Meier, K. K.; Tian, S. L.; Zhang, J. L.; Guo, H. C.; Schulz, C. E.; Robinson, H.; Nilges, M. J.; Munck, E.; Lu, Y. *J. Am. Chem. Soc.* **2014**, *136*, 12337.
- (35) Bhagi-Damodaran, A.; Petrik, I. D.; Marshall, N. M.; Robinson, H.; Lu, Y. *J. Am. Chem. Soc.* **2014**, *136*, 11882.
- (36) Liu, J.; Chakraborty, S.; Hosseinzadeh, P.; Yu, Y.; Tian, S.; Petrik, I.; Bhagi, A.; Lu, Y. *Chem. Rev.* **2014**, *114*, 4366.
- (37) Gaetke, L. M.; Chow, C. K. *Toxicology* **2003**, *189*, 147.
- (38) Minnihan, E. C.; Young, D. D.; Schultz, P. G.; Stubbe, J. *J. Am. Chem. Soc.* **2011**, *133*, 15942.
- (39) Alfanta, L.; Zhang, Z. W.; Uryu, S.; Loo, J. A.; Schultz, P. G. *J. Am. Chem. Soc.* **2003**, *125*, 14662.
- (40) Liu, X. H.; Jiang, L.; Li, J. S.; Wang, L.; Yu, Y.; Zhou, Q.; Lv, X.; Gong, W.; Lu, Y.; Wang, J. *J. Am. Chem. Soc.* **2014**, *136*, 13094.
- (41) Liu, X. H.; Li, J.; Dong, J.; Hu, C.; Gong, W.; Wang, J. *Angew. Chem. Int. Ed.* **2012**, *51*, 10261.
- (42) Rae, T. D.; Schmidt, P. J.; Pufahl, R. A.; Culotta, V. C.; O'Halloran, T. V. *Science* **1999**, *284*, 805.
- (43) Hastings, G.; Kleinherenbrink, F. A. M.; Lin, S.; McHugh, T. J.; Blankenship, R. E. *Biochemistry* **1994**, *33*, 3193.
- (44) Dunnivant, F. M.; Schwarzenbach, R. P.; Macalady, D. L. *Environ. Sci. Technol.* **1992**, *26*, 2133.
- (45) Tsao, M. L.; Summerer, D.; Ryu, Y.; Schultz, P. G. *J. Am. Chem. Soc.* **2006**, *128*, 4572.
- (46) Peters, F. B.; Brock, A.; Wang, J.; Schultz, P. G. *Chem. Biol.* **2009**, *16*, 148.
- (47) Wang, Y. S.; Fang, X.; Chen, H. Y.; Wu, B.; Wang, Z. U.; Hilty, C.; Liu, W. R. *ACS Chem. Biol.* **2013**, *8*, 405.
- (48) Vergne, C.; BoisChoussy, M.; Ouazzani, J.; Beugelmans, R.; Zhu, J. P. *Tetrahedron: Asymmetry* **1997**, *8*, 391.
- (49) Wang, J.; Zhang, W.; Song, W.; Wang, Y.; Yu, Z.; Li, J.; Wu, M.; Wang, L.; Zang, J.; Lin, Q. *J. Am. Chem. Soc.* **2010**, *132*, 14812.
- (50) Kennis, J. T.; Larsen, D. S.; van Stokkum, I. H.; Vengris, M.; van Thor, J. J.; van Grondelle, R. *Proc. Natl. Acad. Sci. U.S.A.* **2004**, *101*, 17988.
- (51) Leiderman, P.; Genosar, L.; Huppert, D.; Shu, X.; Remington, S. J.; Solntsev, K. M.; Tolbert, L. M. *Biochemistry* **2007**, *46*, 12026.
- (52) Shi, X.; Abbyad, P.; Shu, X.; Kallio, K.; Kanchanawong, P.; Childs, W.; Remington, S. J.; Boxer, S. G. *Biochemistry* **2007**, *46*, 12014.
- (53) Kennis, J. T. M.; van Stokkum, I. H. M.; Peterson, D. S.; Pandit, A.; Wachter, R. M. *J. Phys. Chem. B* **2013**, *117*, 11134.
- (54) van Wilderen, L. J. G. W.; Lincoln, C. N.; van Thor, J. J. *PLoS One* **2011**, *6*, e17373.
- (55) Compton, R. G.; Dryfe, R. A. W.; Fisher, A. C. *J. Chem. Soc., Perk. Trans.* **1994**, 1581.
- (56) Hay, S.; Wallace, B. B.; Smith, T. A.; Ghiggino, K. P.; Wydryzynski, T. *Proc. Natl. Acad. Sci. U.S.A.* **2004**, *101*, 17675.
- (57) Gray, H. B.; Winkler, J. R. *Biochim. Biophys. Acta* **2010**, *1797*, 1563.
- (58) Page, C. C.; Moser, C. C.; Chen, X. X.; Dutton, P. L. *Nature* **1999**, *402*, 47.
- (59) Marcus, R. A. *J. Chem. Phys.* **1956**, *24*, 966.
- (60) Gray, H. B.; Winkler, J. R. *Q. Rev. Biophys.* **2003**, *36*, 341.
- (61) Hu, C.; Chan, S. I.; Sawyer, E. B.; Yu, Y.; Wang, J. Y. *Chem. Soc. Rev.* **2014**, *43*, 6498.